Design of Signed Powers-of-Two Coefficient Perfect Reconstruction QMF Bank Using CORDIC Algorithms

Sang Yoon Park and Nam Ik Cho

***Abstract*—Lattice structures have several advantages over the tapped delay line form, especially for the hardware implementation of general digital filters. It is also efficient for the implementation of quadrature mirror filter (QMF), because the perfect reconstruction is preserved under the coefficient quantization. Moreover, if lattice coefficients are implemented in signed powers-of-two (SPT), the hardware complexity can also be reduced. But the discrete coefficient space with the SPT representation is sparse when the number of nonzero bits is small. This paper proposes a structure of orthogonal QMF lattice with SPT coefficients, which has much denser discrete coefficient space than the conventional structure. While the conventional approaches directly quantize the lattice coefficients into SPT form, the proposed algorithm considers the quantization in the SPT angle space. For this, each lattice stage is implemented by the cascade of several variants of COordinate Rotation DIgital Computer. The resulting angle space and corresponding discrete coefficient space is much denser than the one generated by the conventional direct quantization approach. An efficient coefficient search algorithm for this structure is also proposed. Since the proposed architecture provides denser coefficient space, it shows less coefficient quantization error than the conventional QMF lattice.**

***Index Terms*—COordinate Rotation DIgital Computer (CORDIC), lattice filter, perfect reconstruction (PR), quadrature mirror filter (QMF), signed powers-of-two (SPT).**

I. Introduction

THE quadrature mirror filter (QMF) bank is used in diverse fields of signal processing, and thus there has been much research on its efficient design and implementation [1]–[12]. One of the most important issues in the design of QMF is perfect reconstruction (PR) property, i.e., the output must be the same as the input when there is no manipulation on the subband signals. It is shown that the QMF in Fig. 1 is a PR system when the analysis filters $H_i(z)$ and synthesis filters $F_i(z)$ constitute the paraunitary (PU) system. Based on this theory, the QMF can be implemented by the repetition of two PU systems, namely, the rotation and delay as shown in Fig. 2(a). Since the rotation is represented as

$$\mathbf{R}_n = \begin{bmatrix} \cos\theta_n & \sin\theta_n \\ -\sin\theta_n & \cos\theta_n \end{bmatrix} = \cos\theta_n \begin{bmatrix} 1 & \alpha_n \\ -\alpha_n & 1 \end{bmatrix}, \quad \text{for} \quad n = 0, 1, \cdots, N \qquad (1)$$

Manuscript received February 15, 2005; revised August 21, 2005. This paper was recommended by Associate Editor B.-D. Liu.

The authors are with the School of Electrical Eng. and Computer Science, and also affiliated with the Institute of New Media and Communications (INMC), Seoul National University, Seoul 151-744, Korea (e-mail: nicho@snu.ac.kr).

Digital Object Identifier 10.1109/TCSI.2006.870478

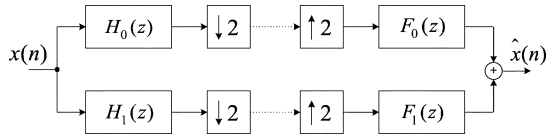

Fig. 1. Two-channel QMF bank.

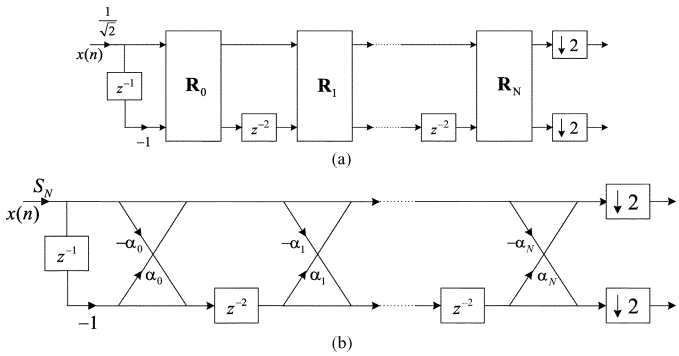

Fig. 2. Analysis bank of two-channel PR QMF lattice filter represented by (a) rotation blocks and (b) real coefficient blocks.

where $\alpha_n = \tan\theta_n$, the overall PR QMF can be implemented in the lattice form as shown in Fig. 2(b). It is well known that this lattice form has several advantages over the direct implementation of $H_i(z)$ and $F_i(z)$ in tapped delay line (TDL) structures. One of the most important properties is that the PR property is satisfied even under the severe quantization of filter coefficients. Another important advantage of the lattice filter in general is that it requires half number of multiplications per unit time (MPU) compared to the TDL implementation [1]. Hence, we attempt to derive a more efficient structure and design methods for the PR QMF lattice by employing COordinate Rotation DIgital Computer (CORDIC) and signed powers-of-two (SPT) representation, which can improve the filtering performance for the given hardware complexity.

When implementing a digital filter, its performance is generally traded with the hardware complexity. For example, quantization of a coefficient by shorter wordlength leads to lower complexity but poorer performance. Another approach to the tradeoff between the performance and complexity is to use the SPT coefficients with the limited number of nonzero digits. For the given wordlength B, each digit can have -1, 0, or $+1$ in the SPT representation. If we limit the number of nonzero digits to M, then the multiplication of input with the SPT coefficient can be implemented by M shifts and $M-1$ adds. Thus, smaller M leads to lower hardware complexity. But when $M < B/2$, it is

not possible to represent all the integers in $[0, 2^B)$, and hence smaller M results in less possible integer representations for each coefficient and poorer filter performance. For designing a filter with the SPT coefficients, the simplest method is to find the optimal coefficients with high precision arithmetic, and then just round the coefficients to the nearest possible SPT representations. But this generally leads to large performance degradation, especially because there are some regions (in the set of $[0, 2^B)$) where possible SPT elements are very sparsely distributed. Hence, many optimal and suboptimal approaches have been introduced for the design of filters in the discrete coefficient space. In the case of designing TDL filters with SPT coefficients, there are optimal design methods such as mixed integer linear programming (MILP) [13]. But the MILP cannot be directly applied to the design of lattice filters, because the frequency response of a filter is not linearly related with its lattice coefficients. Hence, the local optimization techniques [6]–[9] or genetic algorithms [10], [11], [15] have been employed for the design of lattice filters with discrete coefficients. These conventional design methods for the SPT PR QMF lattice are focused on finding the optimal coefficients of a given structure, not on the improvement of structure. In this paper, we propose a new architecture for the performance improvement of lattice PR QMF without increasing hardware complexity. More specifically, we find a structure that can give larger numbers of possible SPT representation for the same constraint B and M. The proposed architecture provides denser coefficient space than the conventional one, while the hardware complexity is the same. As a result, the quantization error of the proposed lattice filter is smaller and the performance is improved.

The proposed architecture is based on the lattice form of Fig. 2(b), where each stage is replaced by various CORDIC processors. If each α_n of Fig. 2(b) is just quantized into SPT representation, then each stage is equivalent to a single CORDIC rotation [12], [16]–[21]. More precisely, let us define $[\cdot]_Q$ as a quantization operator and if a lattice coefficient α_n is quantized into the SPT form as

$$[\alpha_n]_Q = \sum_{k=1}^{M} s_{k,n} 2^{-p_{k,n}}, \qquad \text{for} \quad n = 0, 1, \cdots, N$$
$$s_{k,n} \in \{-1, 1\}, \quad p_{k,n} \in \{-2, -1, 0, 1, \cdots, B\} \tag{2}$$

with $M = 1$ (the coefficient is quantized into SPT form with a single nonzero digit.), then it is just a modified vector rotational (MVR) CORDIC [18], [20]. If $M = 2$ (the coefficient is quantized into SPT with two nonzero digits), then a lattice stage is equivalent to the extended elementary angle set (EEAS) CORDIC [19], [20]. With this key feature of the architecture, we propose two techniques for increasing the density of discrete coefficient space: The first is to replace each lattice stage by the cascade of CORDIC subrotations, whereas the conventional design considers only a single subrotation (i.e., just direct quantization of a lattice coefficient). For the case of $M = 2$, this means we can use the cascade of two MVR-CORDICs as well as EEAS-CORDIC, which provides about two times denser distribution of possible coefficients than the conventional SPT. The second technique is to add $\pi/2 + \theta$ and $\pi/2 - \theta$ into the list of candidate angles when the θ is a candidate. This provides about 1.5 times more possible SPT coefficients. As a result, the number of possible coefficients are tripled without additional hardwares. Moreover, when $M > 2$, it provides much more possible representations. It is also verified that the proposed scheme provides more uniform distribution of possible points in the discrete coefficient space, which is an additional advantage.

As stated previously, it is almost impossible to find the optimal discrete coefficients of a lattice filter. Hence, the conventional design algorithms were based on the sub-optimal techniques such as local search [6]–[8] and genetic algorithm [10], [11], [15]. Although these techniques provide reasonable results, they have some drawbacks. Specifically, the local search techniques apt to fall into a local optima near the initial points, and the genetic approaches require a large number of iterations to find a solution. Hence, we propose a design technique that is the combination of these two approaches. They are combined to compensate for each other's disadvantage, and thus we can have final suboptimal result with less iterations.

The paper is organized as follows. We briefly summarize the PR QMF lattice and its relationship with CORDIC architecture in Section II. In Section III, we first analyze the quantization error of lattice subrotation and show that the reduction of angle approximation error is more important than the roundoff error. That is, the coefficient quantization error is more serious than the roundoff error when the number of nonzero digits is small, and this is why we try to increase the density of coefficient space rather than just increase the wordlength. A coefficient optimization method is also proposed in this section. In Section IV, design examples are shown to demonstrate the performance improvement. Finally, conclusions are given in Section V.

II. PR QMF Lattice and CORDIC Algorithms

A. Review of PR QMF Lattice

Fig. 1 shows a two-channel maximally decimated QMF bank. Assuming no degradation in the channel, if the reconstructed signal $\hat{x}(n)$ is related with the input $x(n)$ as

$$\hat{x}(n) = c \cdot x(n - 2N - 1) \tag{3}$$

for some integer N and scalar c, then the filter bank is called PR system. The PR QMF bank can also be factorized into cascades of PU *Givens* rotation $\mathbf{R}_n$ and delay blocks as shown in Fig. 2(a) [1], [2]. If we implement the rotator as in (1) for reducing hardware cost, the analysis filter is represented as

$$\begin{bmatrix} H_0(z) \\ H_1(z) \end{bmatrix} = S_N \mathbf{L}_N \mathbf{\Lambda}(z^2) \mathbf{L}_{N-1} \mathbf{\Lambda}(z^2) \cdots \mathbf{\Lambda}(z^2) \mathbf{L}_n \mathbf{\Lambda}(z^2) \cdots \mathbf{\Lambda}(z^2) \mathbf{L}_0 \begin{bmatrix} 1 \\ -z^{-1} \end{bmatrix} \tag{4}$$

where

$$\mathbf{L}_n = \begin{bmatrix} 1 & \alpha_n \\ -\alpha_n & 1 \end{bmatrix}$$
$$\mathbf{\Lambda}(z) = \begin{bmatrix} 1 & 0 \\ 0 & z^{-1} \end{bmatrix} \tag{5}$$
$$S_N = \frac{1}{\sqrt{2}} \prod_{n=0}^{N} \frac{1}{\sqrt{1 + \alpha_n^2}}. \tag{6}$$

For the hardware implementation of QMF, the coefficients are quantized to an element in a set of finite integers. Then, the PR property does not hold any more in the case of TDL implementation. However, in the case of lattice structure of Fig. 2(b), the PR is preserved under the quantization [1], [2].

B. Review of CORDIC and Modified CORDIC

In conventional approaches to the SPT implementation of lattice filters [6]–[11], a set of integers represented by SPT with given B and M is prepared. Then the (sub)optimal search algorithm finds an appropriate element to each coefficient for the given frequency response. But, since each stage of QMF lattice is a rotational operation, it can also be implemented by CORDIC algorithm. The proposed architecture is based on this CORDIC implementation with small number of subrotations. There are many kinds of CORDIC algorithms that can be used for this purpose, and some of them are actually equivalent to the conventional SPT lattice filter. In this subsection, we briefly review the CORDIC and modified CORDIC algorithms.

In the CORDIC algorithm, a given vector rotation is decomposed into a series of incremental subrotations, where each subrotation is implemented by only two shift/add operations [16], [17]. More precisely, the basic rotation matrix with the angle θ is decomposed into the subrotation matrices as

$$\begin{aligned}\begin{bmatrix}\cos\theta & \sin\theta\\ -\sin\theta & \cos\theta\end{bmatrix} &= \prod_{i=0}^{S-1}\begin{bmatrix}\cos\sigma_i a_i & \sin\sigma_i a_i\\ -\sin\sigma_i a_i & \cos\sigma_i a_i\end{bmatrix}\\ &= K\prod_{i=0}^{S-1}\begin{bmatrix}1 & \sigma_i 2^{-i}\\ -\sigma_i 2^{-i} & 1\end{bmatrix}\end{aligned} \tag{7}$$

where S is the number of subrotations, σ_i is a sequence of ± 1, and K and a_i are defined as

$$a_i \triangleq \tan^{-1}(2^{-i}), \qquad K \triangleq \prod_{i=0}^{S-1}\frac{1}{\sqrt{1+2^{-2i}}}. \tag{8}$$

Fig. 3 shows an example that a stage of QMF lattice in Fig. 2(a) is replaced by CORDIC.

There have also been some researches on the modification of CORDIC for improving the accuracy, complexity, and speed of computation. The main difference of these modified algorithms from the conventional scheme is that the elementary rotation angle a_i is expanded in a more flexible way. That is, we can have more elementary angles by modifying (7) and (8) as

$$\begin{aligned}a_i &\triangleq \tan^{-1}\left(\sum_{k=1}^{M} s_{k,i}2^{-p_{k,i}}\right)\\ K &\triangleq \prod_{i=0}^{S-1}\frac{1}{\sqrt{1+\left(\sum_{k=1}^{M} s_{k,i}2^{-p_{k,i}}\right)^2}},\\ s_{k,i} &\in \{-1,1\}; \quad p_{k,i} \in \{-2,-1,0,1,\cdots,B\}\end{aligned} \tag{9}$$

while the number of iterations S is fixed to a predetermined value (usually 2 or 3) that is less than the wordlength B, and $\sigma_i = 1$. From these equations, we can see that $\tan(a_i)$ is the $[\alpha_n]_Q$ in (2). The modified CORDIC algorithms are named as follows, according to the parameter M:

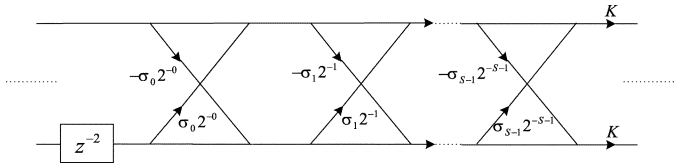

Fig. 3. Stage of the QMF lattice implemented by the CORDIC.

$$\begin{aligned}M=1:&\quad \text{MVR}-\text{CORDIC [18]}\\ M=2:&\quad \text{EEAS}-\text{CORDIC [19]}\\ M\geq 3:&\quad \text{Generalized EEAS}-\text{CORDIC [19]}.\end{aligned} \tag{10}$$

C. Relationship Between the CORDIC and QMF Lattice With SPT Coefficients

In this subsection, we show the relationship between CORDIC and QMF lattice with SPT coefficients. As stated previously, implementing a rotation $\mathbf{R}_n$ in Fig. 2(a) by CORDIC is sometimes equivalent to the implementation of lattice filter in Fig. 2(b) with the SPT coefficients. If we implement $\mathbf{R}_n$ by MVR-CORDIC with $S = 1$, it is equivalent to quantizing α_n into SPT with a single nonzero digit. If $\mathbf{R}_n$ is implemented by EEAS-CORDIC with $S = 1$, it is equivalent to quantizing α_n into SPT with two nonzero digits. Generalized EEAS-CORDIC where $M \geq 3$ can also be similarly compared with the direct SPT quantization. In other words, when $S = 1$, M is the number of nonzero digits in SPT representation.

It is well known that these CORDIC structures entail the irregular scaling factor, which is denoted by K as in (9). Hence, the scaling factor should be taken into consideration when implementing the rotation $\mathbf{R}_n$ by MVR or EEAS-CORDIC. From the relationship between the modified CORDICs and the QMF lattice, it can be seen that the scaling factor K is directly related with that of QMF lattice S_N in (6). More specifically, if we define K_n as the scaling factor introduced at the nth stage of the lattice, it can be represented as

$$K_n \triangleq \frac{1}{\sqrt{1+\left(\sum_{k=1}^{M} s_{k,n}2^{-p_{k,n}}\right)^2}} \tag{11}$$

from (9). Then, the scaling factor of the Nth-order lattice filter can be written as

$$\prod_{n=0}^{N} K_n = \prod_{n=0}^{N}\frac{1}{\sqrt{1+\left(\sum_{k=1}^{M} s_{k,n}2^{-p_{k,n}}\right)^2}} \tag{12}$$

which is equivalent to (6) with the α_n replaced by (2) except for the constant multiplication of $1/\sqrt{2}$. From these relationship, the S_N can be calculated using the scaling factors of modified CORDICs as

$$S_N = \frac{1}{\sqrt{2}}\prod_{n=0}^{N} K_n. \tag{13}$$

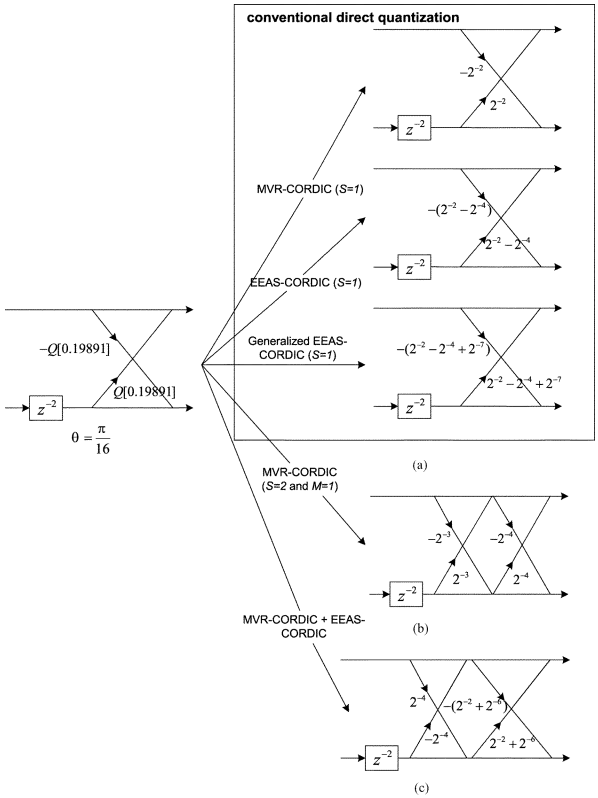

Fig. 4. Example of implementing a subrotation of QMF lattice by modified CORDICs. (a) Subrotation angle $\theta = \pi/16$ is quantized into $S = 1$ and $M = 1, 2, 3$. (b) Example of $S = 2$, $M = 1$. (c) Combination of MVR and EEAS-CORDIC.

Fig. 4(a) shows an example that a subrotation of QMF lattice with $\theta = \pi/16$ is approximated by the modified CORDICs. As shown in the figure, they are equivalent to a lattice filter where the coefficient $0.19891(= \tan^{-1}\pi/16)$ is quantized into SPT form with one, two, or three nonzero digits. And these are equivalent to the modified CORDICs with $S = 1$, and $M = 1, 2, 3$, respectively, which usually have non-uniform and limited numbers of possible angles. The main idea of this paper is to increase the number of possible angles and improve the non-uniformity by using other modified CORDIC structures. That is, instead of the conventional SPT lattice with $M = 2$, which is equivalent to the EEAS-CORDIC with $S = 1$ and $M = 2$ [second CORDIC in Fig. 4(a)], we use $S = 2$ and $M = 1$ [Fig. 4(b)]. Also, instead of a single rotation represented by 3 nonzero digits (conventional SPT lattice with $M = 3$), we use a cascade of MVR and EEAS-CORDIC [Fig. 4(c)]. This cascade structure with additional definition of angles gives increased number of possible rotations as will be shown later.

III. Proposed PR QMF Lattice Based on the CORDIC

When implementing a vector rotation by a CORDIC with finite set of rotation angles, there are two major error sources, namely angle approximation and roundoff error [23], [24]. In this section, we first show that the angle approximation error is generally larger than the roundoff error in the CORDIC implementation of QMF bank, when M is small. Hence, for the given hardware resources (for the given nonzero digits), increasing the number of possible rotation angles is more important than just increasing the wordlength B. Based on this observation, we propose two techniques that can increase the density of coefficient space for the given B and M. We also show that possible SPT coefficients of the proposed method are more evenly distributed over the discrete space. An optimization technique for finding suboptimal SPT coefficients is also proposed in this section.

A. Coefficient Quantization Error of PR QMF Lattice

In this subsection, we evaluate the angle approximation and roundoff error of a single lattice stage when the lattice coefficient is directly quantized into SPT form. The angle approximation error is introduced by the residual angle δ, which results from the rounding of a given rotational angle θ to one of predefined finite elementary angles as [20], [23]

$$\delta \triangleq \theta - \sum_{i=0}^{S-1} \tan^{-1}\left(\sum_{k=1}^{M} s_{k,i} 2^{-p_{k,i}}\right). \tag{14}$$

If the residual angle is known, then the variance of angle approximation error can be estimated as [23]

$$E|\mathbf{e}_{\text{angle}}|^2 \simeq \delta^2 \cdot E|\mathbf{v}|^2 \tag{15}$$

where $|\mathbf{v}|^2$ is the input energy of the stage.

The roundoff error is introduced when performing the shift operation in (7). If the multiplication is replaced by a right-shift, then the roundoff error is uniformly distributed over $[-2^{-B-1}, 2^{-B-1}]$. Thus, the total roundoff error $E|\mathbf{e}_{\text{round}}|^2$ can be evaluated as a sum of variance and square of mean [23]

$$\begin{aligned} E|\mathbf{e}_{\text{round}}|^2 &= 2K^2\left[\sum_{k=1}^{M} w(p_{k,S-1}) + \sum_{j=1}^{S-1}\left(\left(\sum_{k=1}^{M} w(p_{k,j-1})\right)\left(\prod_{i=j}^{S-1} k(i)^2\right)\right)\right] \\ &\quad + K^2\left|E\{\mathbf{e}_{\text{round}}(S)\} + \sum_{j=1}^{S-1} \widetilde{\mathbf{P}}(j) E\{\mathbf{e}_{\text{round}}(j)\}\right|^2 \end{aligned} \tag{16}$$

where

$$\widetilde{\mathbf{P}}(j) = \prod_{i=j}^{S-1}\begin{bmatrix} 1 & \sum_{k=1}^{M} s_{k,i} 2^{-p_{k,i}} \\ -\sum_{k=1}^{M} s_{k,i} 2^{-p_{k,i}} & 1 \end{bmatrix}$$

$$k(i) = \sqrt{1 + \left(\sum_{k=1}^{M} s_{k,i} 2^{-p_{k,i}}\right)^2},$$

$$w(p_{k,i}) = \frac{2^{-2B}}{12}(1 - 2^{-2p_{k,i}}), \text{ and}$$

$$E\{\mathbf{e}_{\text{round}}(j)\} = \sum_{k=1}^{M}\left(s_{k,j-1} \cdot 2^{-B-1}(2^{-p_{k,j-1}} - 1)\right)\begin{bmatrix} 1 \\ -1 \end{bmatrix}. \tag{17}$$

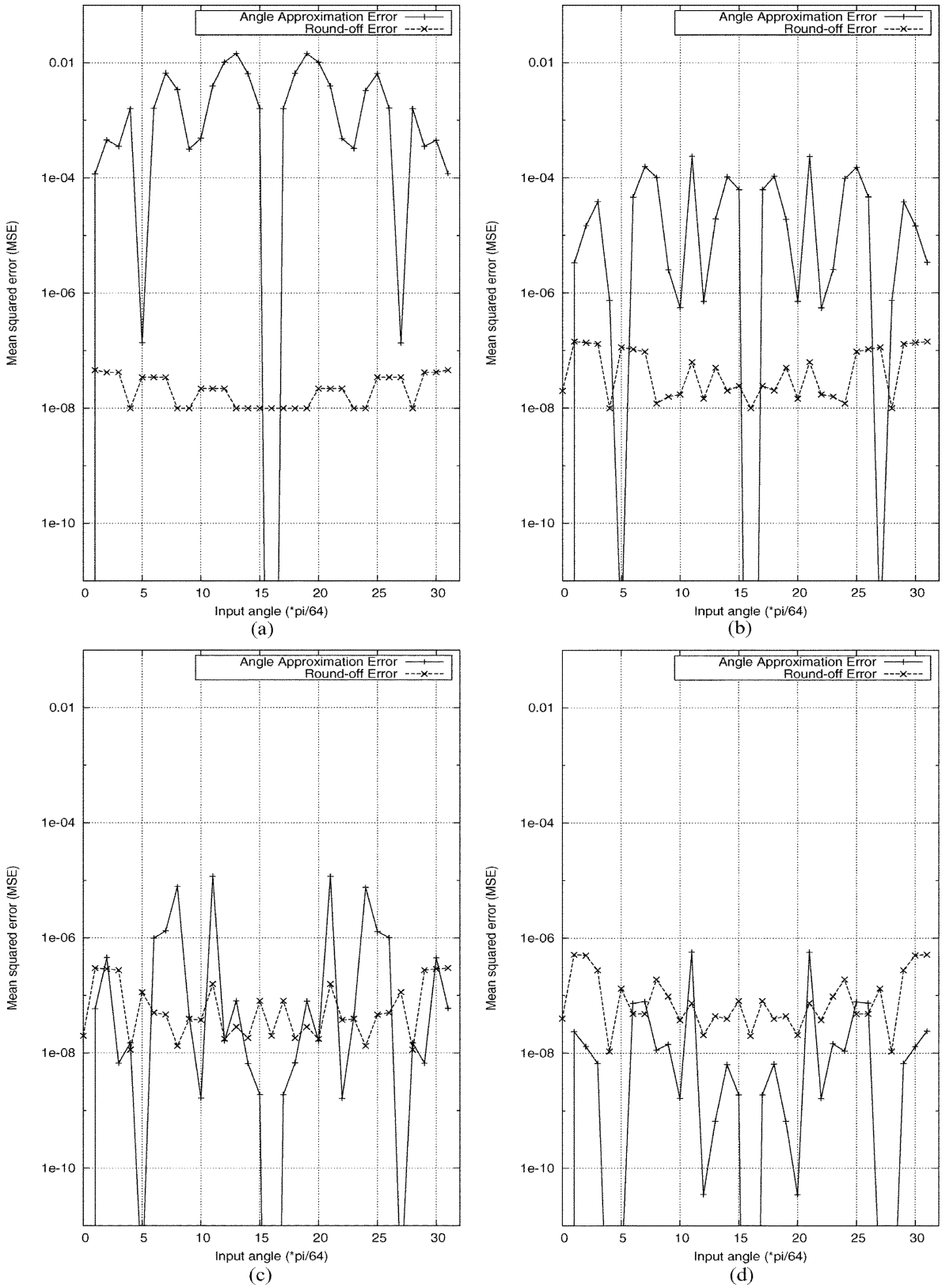

Fig. 5. Comparison of angle approximation error and roundoff error ($B = 11$). (a) MVR-CORDIC ($S = M = 1$). (b) EEAS-CORDIC ($S = 1, M = 2$). (c) Generalized EEAS-CORDIC ($S = 1, M = 3$). (d) Generalized EEAS-CORDIC ($S = 1, M = 4$).

The parameters $s_{k,i}$ and $p_{k,i}$ can be pre-calculated in this case, because the subrotation angle is known in advance. Hence, the angle approximation and roundoff error can be easily estimated.

Based on this error analysis, we evaluate the angle approximation and roundoff errors for the conventional SPT design of Fig. 4(a) ($S = 1, M = 1, 2, 3, 4$). The results for $B = 11$

are compared in Fig. 5 in order to see which error source is more serious. It can be observed that the angle approximation error decreases significantly as M increases, whereas the accumulated roundoff error remains almost the same. Hence, the angle approximation is a dominant error source when $M < 4$, and vice versa. Increasing S with fixed M yields the same tendency, though the result is not shown here. In summary, when the $S \times M$ (number of nonzero digits in a stage) is less than 4, the angle approximation is a dominant error source, to which more attention have to be paid. Meanwhile, as B gets smaller, the roundoff error may increase. However, if B is not too small, the angle approximation error remains as a considerable error source. Specifically, when $S = 1$ and $M = 3$, B less than 7 introduces the roundoff error that is ten times larger than the angle approximation error (Note that B is usually larger than 7 in practical design for obtaining a comparable performance with the ideal design.). For the reduction of angle approximation error, the discrete angle space should be more dense. And the most straightforward approach to increasing the density of angle space is to increase the nonzero digits M and/or the wordlength B. But the increase of B and/or M results in increased hardware complexity. Hence, in this paper, we try to find a new structure that provides more dense coefficient space than the conventional SPT lattice filters, for the given B and M.

B. Design of Proposed PR QMF Lattice

As stated previously, Fig. 4(a) illustrates the conventional approach that a lattice coefficient is quantized into SPT representations with one, two, or three nonzero digits. It also shows that they correspond to MVR-CORDIC ($S = M = 1$), EEAS-CORDIC ($S = 1$, $M = 2$), and generalized EEAS-CORDIC ($S = 1$, $M = 3$). The main idea of the proposed approach is to increase possible rotation angles by splitting the latter two cases into the cascades of elementary rotations as shown in Fig. 4(b) and (c). In this subsection, we show how many rotation angles are increased by this cascade structure, and also propose a method to further increase the angles. The distribution of these angles over the discrete coefficient space is also discussed.

Table I (a) shows the conventional SPT representation of the lattice coefficient with two nonzero digits [6]–[10]. If θ_n is the angle of lattice coefficients designed in high precision arithmetic, it can be quantized into finite precision value as

$$[\theta_n]_Q = \tan^{-1}(s_1 2^{-p_1} + s_2 2^{-p_2}). \tag{18}$$

In addition to the angles obtained by this conventional structure, we can have more angles by using following two methods. The first method is to split one rotation (when $M > 2$) into several subrotations. Table I (b) is the structure that replaces this conventional scheme, which is actually an MVR-CORDIC with $S = 2$ and $M = 1$, that is,

$$[\theta_n]_Q = \tan^{-1}(s_1 2^{-p_1}) + \tan^{-1}(s_2 2^{-p_2}). \tag{19}$$

It can provide new rotation angles that cannot be generated by the conventional structure in (a), while it uses the same number of shift/add operations. Thus, considering both (a) and (b)

TABLE I
STRUCTURES FOR STAGE OF QMF LATTICE IN SPT DOMAIN FOR CASE OF $M = 2$

	Lattice Structure	Angle
(a)	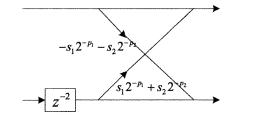	$\tan^{-1}(s_1 2^{-p_1} + s_2 2^{-p_2})$
(b)	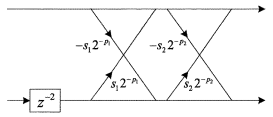	$\tan^{-1}(s_1 2^{-p_1}) + \tan^{-1}(s_2 2^{-p_2})$
(c)	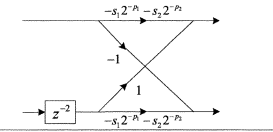	$\tan^{-1}(s_1 2^{-p_1} + s_2 2^{-p_2}) + \frac{\pi}{2}$
(d)	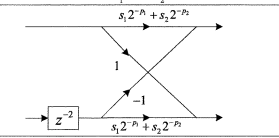	$\tan^{-1}(s_1 2^{-p_1} + s_2 2^{-p_2}) - \frac{\pi}{2}$
(e)	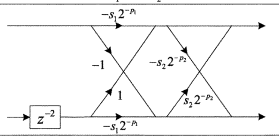	$\tan^{-1}(s_1 2^{-p_1}) + \tan^{-1}(s_2 2^{-p_2}) + \frac{\pi}{2}$
(f)	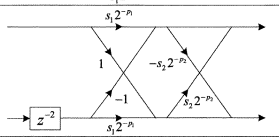	$\tan^{-1}(s_1 2^{-p_1}) + \tan^{-1}(s_2 2^{-p_2}) - \frac{\pi}{2}$

during the quantization process, this extension provides about two times denser distribution than the conventional SPT. The second method is to rotate the angles of (18) and (19) by $\pm\pi/2$, that is

$$[\theta_n]_Q = \tan^{-1}(s_1 2^{-p_1} + s_2 2^{-p_2}) \pm \frac{\pi}{2} \tag{20}$$

$$[\theta_n]_Q = \tan^{-1}(s_1 2^{-p_1}) + \tan^{-1}(s_2 2^{-p_2}) \pm \frac{\pi}{2}. \tag{21}$$

For the derivation of modified CORDIC structure that reflects this rotation of angles, let us first consider the following factorizations:

$$\begin{bmatrix} \cos\left(\theta_n + \frac{\pi}{2}\right) & \sin\left(\theta_n + \frac{\pi}{2}\right) \\ -\sin\left(\theta_n + \frac{\pi}{2}\right) & \cos\left(\theta_n + \frac{\pi}{2}\right) \end{bmatrix} = \cos\theta_n \begin{bmatrix} -\alpha_n & 1 \\ -1 & -\alpha_n \end{bmatrix}$$
$$\begin{bmatrix} \cos\left(\theta_n - \frac{\pi}{2}\right) & \sin\left(\theta_n - \frac{\pi}{2}\right) \\ -\sin\left(\theta_n - \frac{\pi}{2}\right) & \cos\left(\theta_n - \frac{\pi}{2}\right) \end{bmatrix} = \cos\theta_n \begin{bmatrix} \alpha_n & -1 \\ 1 & \alpha_n \end{bmatrix} \tag{22}$$

where $\theta_n = \tan^{-1}\alpha_n$. Based on this factorization, it can be easily shown that the structures with rotated angles can be represented by the ones in Table I (c)–(f). In summary, the proposed method is to consider all the structures in Table I at the same time, whereas the conventional methods consider only the structure of (a). It seems that the proposed structure provides six times denser distribution than the conventional one because there are six cases in Table I. However, since the angle should be restricted to $[-\pi/2, \pi/2]$ and there are some redundant angles, the number of actual possible angles is less than expected. Fig. 6(a) shows the number of coefficients in the conventional [Table I (a)], proposed design 1 [considering Table I (a) and (b)],

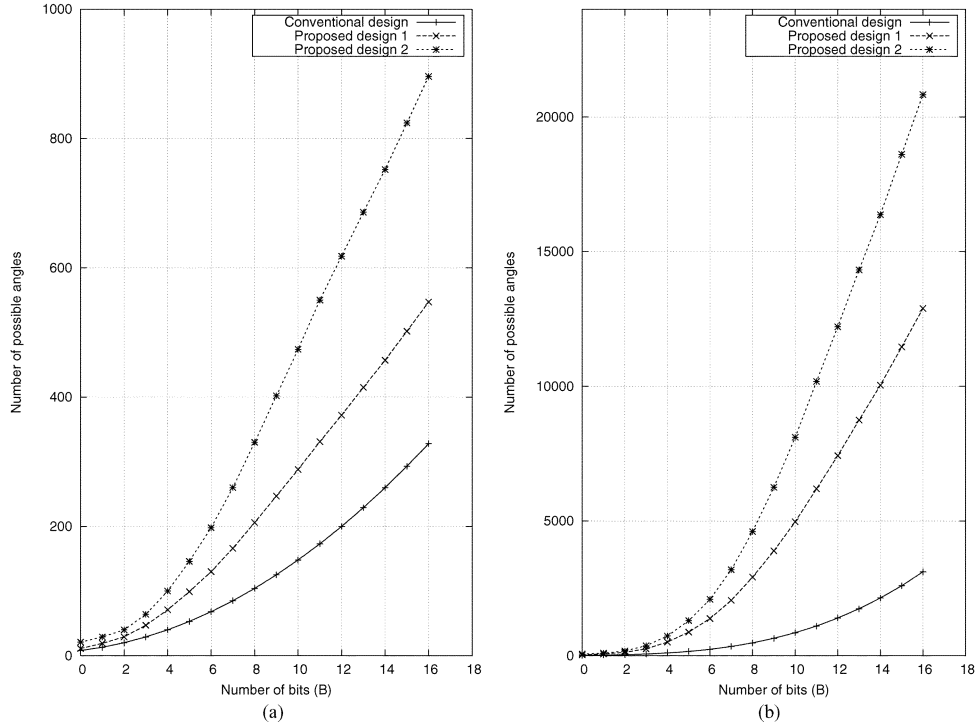

Fig. 6. Number of possible angles when $[\theta_n]_Q \geq 0$. (a) $\mathrm{M} = 2$. (b) $\mathrm{M} = 3$.

TABLE II
POSSIBLE ROTATION ANGLES FOR THE CASE OF $M = 3$

	Angle
(a)	$\tan^{-1}(s_1 2^{-p_1} + s_2 2^{-p_2} + s_3 2^{-p_3})$
(b)	$\tan^{-1}(s_1 2^{-p_1}) + \tan^{-1}(s_2 2^{-p_2}) + \tan^{-1}(s_3 2^{-p_3})$
(c)	$\tan^{-1}(s_2 2^{-p_2} + s_3 2^{-p_3}) + \tan^{-1}(s_1 2^{-p_1})$
(d)	$\tan^{-1}(s_1 2^{-p_1} + s_3 2^{-p_3}) + \tan^{-1}(s_2 2^{-p_2})$
(e)	$\tan^{-1}(s_1 2^{-p_1} + s_2 2^{-p_2}) + \tan^{-1}(s_3 2^{-p_3})$
(f)	$\tan^{-1}(s_1 2^{-p_1} + s_2 2^{-p_2} + s_3 2^{-p_3}) \pm \frac{\pi}{2}$
(g)	$\tan^{-1}(s_1 2^{-p_1}) + \tan^{-1}(s_2 2^{-p_2}) + \tan^{-1}(s_3 2^{-p_3}) \pm \frac{\pi}{2}$
(h)	$\tan^{-1}(s_2 2^{-p_2} + s_3 2^{-p_3}) + \tan^{-1}(s_1 2^{-p_1}) \pm \frac{\pi}{2}$
(i)	$\tan^{-1}(s_1 2^{-p_1} + s_3 2^{-p_3}) + \tan^{-1}(s_2 2^{-p_2}) \pm \frac{\pi}{2}$
(j)	$\tan^{-1}(s_1 2^{-p_1} + s_2 2^{-p_2}) + \tan^{-1}(s_3 2^{-p_3}) \pm \frac{\pi}{2}$

and proposed design 2 [considering all the structures in Table I (a)–(f)] when the rotation angle is larger than 0.

For the case of $M = 3$, it is possible to use more diverse combinations of cascades. Table II shows all the possible rotation angles for $M = 3$, where Table II (a) is the rotation angle of the conventional SPT lattice, and (b) is the rotation angle based on the MVR-CORDIC ($S = 3$ and $M = 1$), which is the extension of Table I (b). Unlike the case of $M = 2$, combination of MVR and EEAS-CORDIC can generate new rotation angles as shown in Table II (c)–(e). This gives completely different angles from the previous ones. Table II (f)–(j) show the structures that $\pm\pi/2$ is added to the rotation angles in (a)–(e). Fig. 6(b) shows the number of coefficients in the conventional [Table II (a)], proposed design 1 [Table II (a)–(e)], and proposed design 2 [Table II (a)–(j)] in the case of $M = 3$. If $M > 3$, the number of elements would increase dramatically.

The proposed scheme implements the rotation of lattice filter by modifying the MVR or EEAS-CORDIC. Hence, the scaling factor in (11) for each structure should also be modified. In this paper, we consider the scaling factors only for the case of $M = 2$, because the scaling factors for $M \geq 3$ can be similarly derived. In the case of the structure of Table I (a), K_n is calculated from (11) with $M = 2$. In the case of Table I (b), the cascade of two subrotations can be represented by the multiplication of two matrices, i.e.,

$$\begin{aligned}&\begin{bmatrix} 1 & s_2 2^{-p_2} \\ -s_2 2^{-p_2} & 1 \end{bmatrix} \begin{bmatrix} 1 & s_1 2^{-p_1} \\ -s_1 2^{-p_1} & 1 \end{bmatrix} \\ &\quad = \left(1 - s_1 s_2 2^{-(p_1+p_2)}\right) \\ &\qquad \times \begin{bmatrix} 1 & \frac{s_1 2^{-p_1} + s_2 2^{-p_2}}{1 - s_1 s_2 2^{-(p_1+p_2)}} \\ -\frac{s_1 2^{-p_1} + s_2 2^{-p_2}}{1 - s_1 s_2 2^{-(p_1+p_2)}} & 1 \end{bmatrix}. \end{aligned} \tag{23}$$

Using (19) and (23), the quantized coefficient can be denoted as

$$\begin{aligned}[\alpha_n]_Q &= \tan\left([\theta_n]_Q\right) \\ &= \tan\left(\tan^{-1}(s_1 2^{-p_1}) + \tan^{-1}(s_2 2^{-p_2})\right) \\ &= \frac{s_1 2^{-p_1} + s_2 2^{-p_2}}{1 - s_1 s_2 2^{-(p_1+p_2)}} \end{aligned} \tag{24}$$

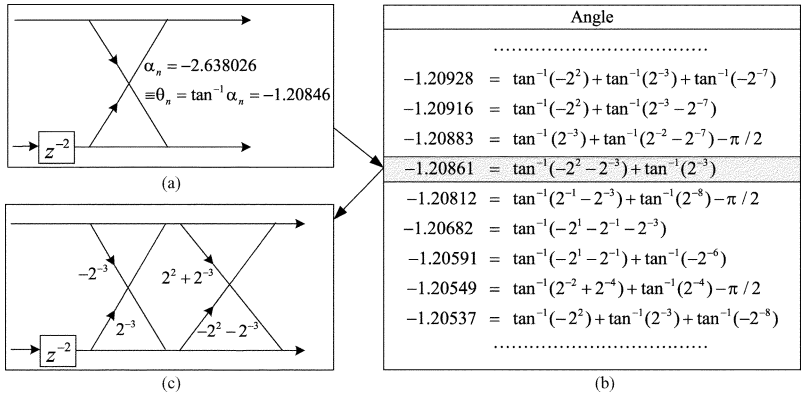

Fig. 7. Angle quantization example.

and K_n is represented as $1/\sqrt{1+[\alpha_n]_Q^2}$. However, we need to consider the scaling factor in the right term of (23), and thus K_n is finally denoted as

$$K_n = \frac{1}{\left(1 - s_1 s_2 2^{-(p_1+p_2)}\right) \cdot \sqrt{1+[\alpha_n]_Q^2}}. \tag{25}$$

In the case of Table I (c)

$$\begin{bmatrix} -s_1 2^{-p_1} - s_2 2^{-p_2} & 1 \\ -1 & -s_1 2^{-p_1} - s_2 2^{-p_2} \end{bmatrix} = -(s_1 2^{-p_1} + s_2 2^{-p_2}) \times \begin{bmatrix} 1 & -\frac{1}{s_1 2^{-p_1} + s_2 2^{-p_2}} \\ \frac{1}{s_1 2^{-p_1} + s_2 2^{-p_2}} & 1 \end{bmatrix}$$

and $[\alpha_n]_Q$ and K_n are represented as

$$\begin{aligned} [\alpha_n]_Q &= \tan\left(\tan^{-1}(s_1 2^{-p_1} + s_2 2^{-p_2}) + \frac{\pi}{2}\right) \\ &= -\frac{1}{s_1 2^{-p_1} + s_2 2^{-p_2}} \\ K_n &= \frac{1}{-(s_1 2^{-p_1} + s_2 2^{-p_2}) \cdot \sqrt{1+[\alpha_n]_Q^2}}. \end{aligned} \tag{26}$$

K_n's of Table I (d)–(f) can also be calculated using a similar factorization technique, and S_N can finally be evaluated by (13). The proposed design does not require any additional hardware for the irregular scaling factors of diverse structures, because we need only a single multiplier for the final constant multiplication of S_N.

Since the proposed architecture is based on CORDIC, we perform the quantization process in the angle domain instead of coefficient domain [20], [21]. For the case of $M = 3$, a simple angle quantization example is demonstrated in Fig. 7. A real coefficient α_n to be quantized is first transformed into the angle θ_n using $arctan$ function as shown in Fig. 7(a). The coefficient candidates are also stored in the form of angle as in Fig. 7(b) in order to proceed all the search processes in the angle domain. If we consider a specific set of $\{s_1, s_2, s_3, p_1, p_2, p_3\}$, then fifteen angles listed according to Table II are stored. If a candidate angle is not in the range of $[-\pi/2, \pi/2]$ or redundant, it is excluded. Fig. 7(b) shows every candidates near the θ_n. From this discrete angle space, we find the (sub)optimal angle for each rotational stages by using local search technique [8] or genetic algorithms [10], [11]. For more efficient search, we may also use the combination of these approaches as will be presented in next subsection. If the coefficient is determined to be -1.20861 as highlighted in Fig. 7(b), then the stage is actually implemented in the form of Fig. 7(c).

The coefficients of a filter can have some specific distribution in some cases. However, it would be desirable to have uniform discrete coefficient space in general. In the case of TDL filter, the SPT coefficient space is very sparse in [1/2, 1] and thus there is a technique to allocate additional nonzero digits to the coefficients larger than 1/2 [14]. This issue is more important in the case of PR QMF lattice, because the distribution of original coefficients is generally wide and uniform. So we need to check the distribution of angle space produced by the proposed scheme. The point is to check whether the angle space is uniform over $[0, \pi/4]$, because most of coefficients are less than 1. Fig. 8(a), (b), and (c) show the angle space produced by conventional direct SPT quantization [Table II (a)], proposed scheme 1 [Table II (a)–(e)], and proposed scheme 2 [Table II (a)–(j)], respectively, in the case of $B = 2$, and $M = 3$. It can be observed that the proposed scheme provides more dense and uniform distribution. Hence, the proposed architecture provides smaller quantization error, especially when the corresponding rotation angle is small. Fig. 8(d) summarizes the density and total number of candidate angles in numbers.

C. Locally Optimized Genetic Algorithm

There is no algorithm that can find the global optimum coefficients for the SPT QMF lattice except for the full search method. Thus, some suboptimal design methods have been proposed, such as the local optimization techniques [6]–[8] or genetic algorithms [10], [11], [15]. The conventional local search technique proposed in [8] provides relatively sharp cutoff response with reasonable amount of computation. However, the final results easily fall into a local optima near the initial point. On the contrary, the genetic approach can provide a solution close to the global optimum by searching a wide range of candidates, but it requires a large number of iterations.

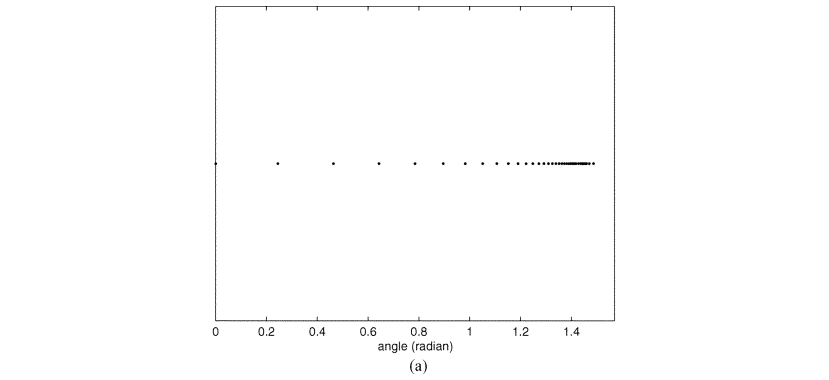

angle (rad)	0.0~0.3	0.3~0.6	0.6~0.9	0.9~1.2	1.2~π / 2	total
conventional	2	1	3	5	25	36
proposed 1	29	17	20	21	37	124
proposed 2	42	26	31	28	47	174

(d)

Fig. 8. Angle distribution of SPT coefficient candidates ($B = 2$ in (2), and $M = 3$). (a) Conventional design [Table II (a)]. (b) Proposed design 1 [Table II (a)–(e)]. (c) Proposed design 2 [Table II (a)–(j)]. (d) The number of possible angles in each region.

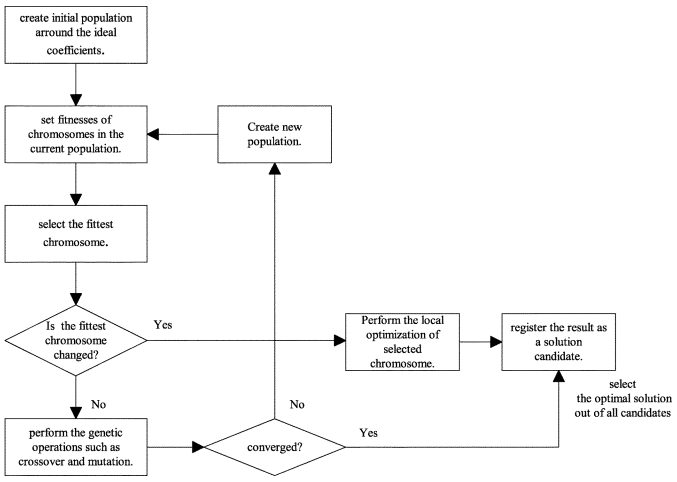

Fig. 9. Block diagram of locally optimized genetic algorithm.

In this paper, we propose an algorithm that is a combination of these two algorithms for increasing the convergence speed. Specifically, Fig. 9 shows the flow chart of the proposed algorithm, which is basically a genetic algorithm [11] with local search [8] inserted in it. As shown in this figure, the fittest member is selected from the current population. If it is different from the fittest member selected in the previous iteration, it is locally optimized and the result is stored as a candidate of solution. After the fitness value converges, the best result is selected from the stored candidates. Since the bivariate local search is performed in the neighborhood of a sub-optimal candidate found by the genetic algorithm, it gives better result than either of local optimization or genetic algorithm. From the extensive design examples, it is found that this approach provides reasonably good design result with small number of iterations.

In the proposed algorithm, the objective function to be minimized is defined as the maximum ripple in the stopband, i.e.,

$$\Phi = \max_{\omega_s \le \omega \le \pi} \left| H_0(e^{j\omega}) \right| \tag{27}$$

where ω_s is the stopband frequency. From the power symmetry property discussed in [1], it also assures the minmax ripple in the passband.

Proposed lattice structure can also be applied to the design of orthogonal wavelet or linear phase QMF lattice. In the case of orthogonal wavelet, additional constraint is needed that the sum of all rotation angles of lattice filter should be $-\pi/4$ [22]. In the case of linear phase QMF lattice, objective function of (27) should be modified to consider the passband ripple as well as the stopband [1], [3]. But these constraints and modifications are not so trivial, and need further studies.

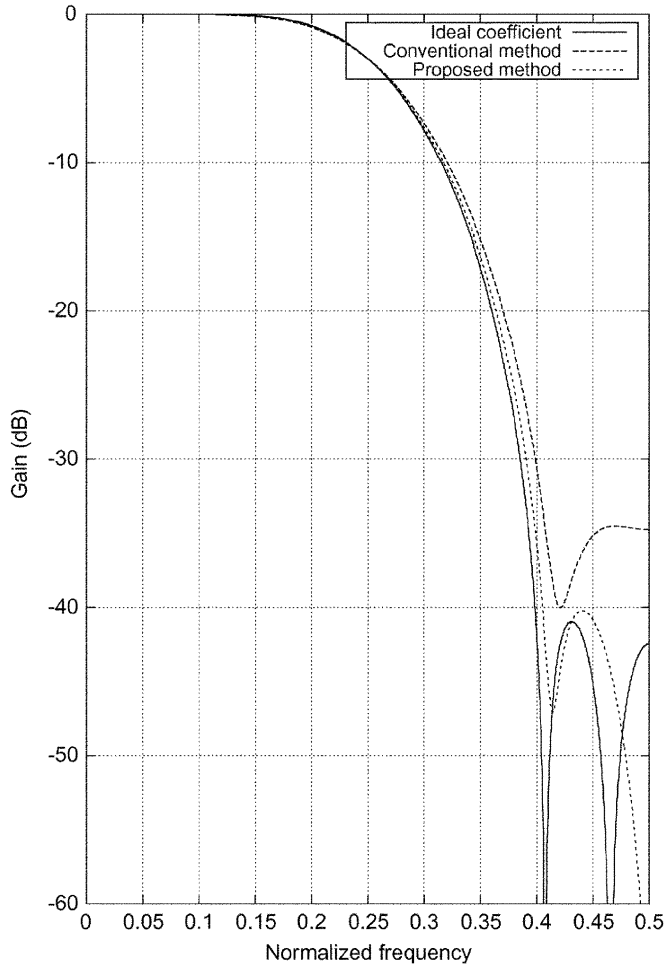

n	ideal α_n	ideal θ_n	quantized θ_n
1	−2.63803	−1.20846	$-1.23150 = \tan^{-1}(-2^{1}) + \tan^{-1}(-2^{-3})$
2	0.71545	0.62102	$0.64350 = \tan^{-1}(-2^{-1}) + \tan^{-1}(-2^{-1}) + \pi/2$
3	−0.25985	−0.25423	$-0.25963 = \tan^{-1}(-2^{-2} - 2^{-6})$
4	0.06388	0.06379	$0.06194 = \tan^{-1}(2^{-3}) + \tan^{-1}(-2^{-4})$

Fig. 10. Frequency response and SPT coefficients for the lowpass filter in the $8A$ filter bank. (conventional method: Table I (a), proposed method: Table I (a)–(f).)

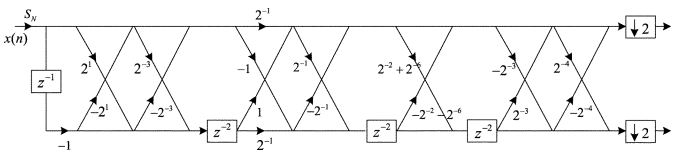

Fig. 11. The analysis bank of the proposed QMF lattice of $8A$.

IV. Design Example

In this section, we present several filter design examples with SPT coefficients. To show the improvement of the proposed design method, the conventional and proposed structure are designed using the same optimization procedure. We first consider "$8A$ filter bank" (with 4 coefficients) defined in [2]. In this example, the minimum value of $p_{k,n}$ is set to -2 to cover enough range of lattice coefficients. We also set the parameters as $B = 8$ and $M = 2$, that is, the wordlength is 11 (from -2 to 8) and there are two nonzero digits. The locally optimized genetic algorithm presented in Section III-C is employed to find the sub-optimal SPT coefficients. Fig. 10 illustrates the frequency responses of the conventional [Table I (a)] and proposed structure [Table I (a)–(f)]. The frequency response of the original QMF (designed in high precision arithmetic) is also shown

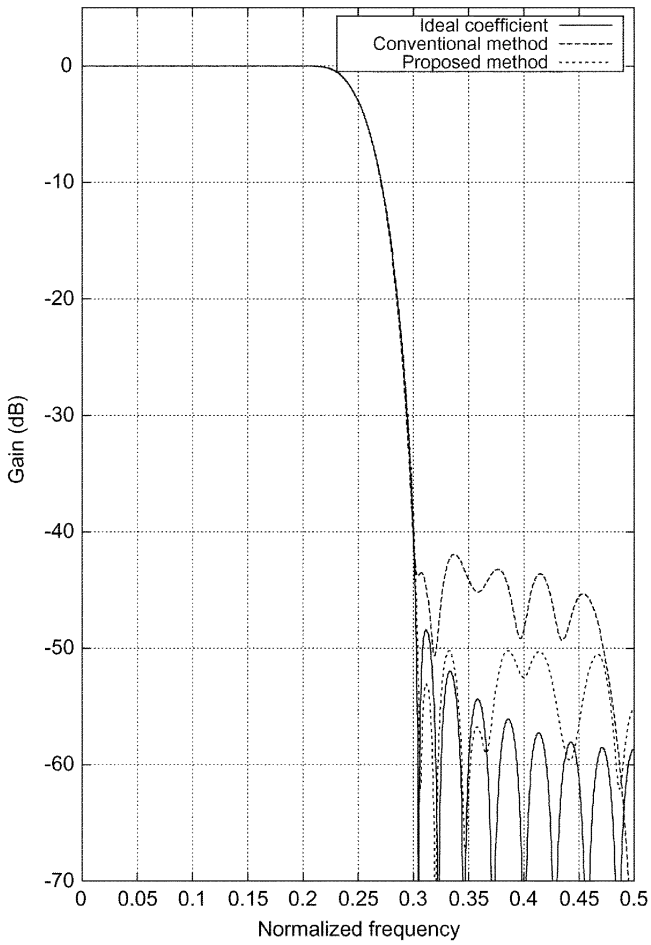

n	ideal α_n	ideal θ_n	quantized θ_n
1	−4.41955	−1.34828	$-1.34763 = \tan^{-1}(2^{-2} - 2^{-5}) + \tan^{-1}(2^{-7}) - \pi/2$
2	1.44487	0.96539	$0.96381 = \tan^{-1}(-2^{2}) + \tan^{-1}(2^{0} - 2^{-3}) + \pi/2$
3	−0.83581	−0.69620	$-0.69387 = \tan^{-1}(-2^{-1}) + \tan^{-1}(-2^{-2} + 2^{-6})$
4	0.56645	0.51538	$0.51349 = \tan^{-1}(2^{-4}) + \tan^{-1}(2^{-1} - 2^{-6})$
5	−0.41109	−0.39003	$-0.38903 = \tan^{-1}(2^{-4}) + \tan^{-1}(2^{1} + 2^{-4}) - \pi/2$
6	0.30798	0.29876	$0.29850 = \tan^{-1}(-2^{2} + 2^{-1} + 2^{-2}) + \pi/2$
7	−0.23342	−0.22931	$-0.22946 = \tan^{-1}(2^{2} + 2^{-2} + 2^{-5}) - \pi/2$
8	0.17649	0.17469	$0.17478 = \tan^{-1}(-2^{2}) + \tan^{-1}(-2^{-4} - 2^{-7}) + \pi$
9	−0.13161	−0.13086	$-0.13190 = \tan^{-1}(-2^{-3} - 2^{-6}) + \tan^{-1}(2^{-7})$
10	0.09573	0.09544	$0.09495 = \tan^{-1}(-2^{-1}) + \tan^{-1}(2^{-1} + 2^{-3})$
11	−0.06712	−0.06702	$-0.06657 = \tan^{-1}(-2^{0}) + \tan^{-1}(2^{0} - 2^{-3})$
12	0.04473	0.04470	$0.04542 = \tan^{-1}(-2^{1}) + \tan^{-1}(2^{1} + 2^{-2})$
13	−0.02782	−0.02781	$-0.02734 = \tan^{-1}(-2^{-6}) + \tan^{-1}(-2^{-7} - 2^{-8})$
14	0.01570	0.01570	$0.01562 = \tan^{-1}(2^{-7}) + \tan^{-1}(2^{-8}) + \tan^{-1}(2^{-}$
15	−0.00765	−0.00765	$-0.00758 = \tan^{-1}(-2^{2}) + \tan^{-1}(2^{2} - 2^{-3})$
16	0.00285	0.00285	$0.00312 = \tan^{-1}(-2^{-1}) + \tan^{-1}(2^{-1} + 2^{-8})$

Fig. 12. Frequency response and SPT coefficients for the lowpass filter in the $32F$ filter bank. (conventional method: Table II (a), proposed method: Table II (a)–(j).)

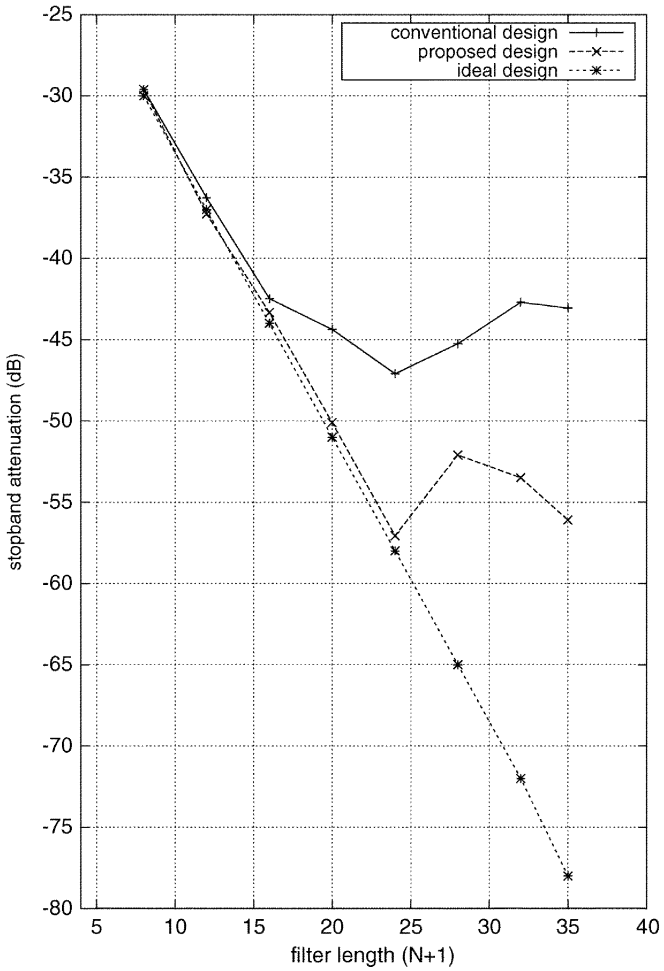

Fig. 13. Stopband attenuation versus filter length.

in the same figure. It can be observed that the ideal coefficient design results in maximum stopband attenuation of 41.0 dB. The stopband attenuation of the proposed design is 40.2 dB, which is 6.0 dB higher than that of the conventional design. The SPT coefficients obtained by the proposed design are listed in Fig. 10, and the corresponding filter is shown in Fig. 11. The complexity of proposed filter bank is almost the same as the conventional one, because each stage of both filter banks can be implemented by four shifters and four adders. As an another design example, $32F$ filter bank (16 coefficients) denoted in [2] is designed. In this example, more nonzero digits are required to get a high stopband attenuation, and thus we set $M = 3$. The frequency response and SPT coefficients for this design are shown in Fig. 12.

Another set of PR QMF banks are also designed in order to show the relationship between the performance and filter length $(N + 1)$ (in Fig. 13). The stopband edge of the lowpass filter is 0.6π, B is set to 12, and M is set to 3. If the filter length is smaller than 16, three designs have similar stopband attenuations proportional to the filter length. However, when the filter length exceeds 16, the stopband ripple of the conventional method shows no change, and the gap between conventional and proposed design increases.

TABLE III
PERFORMANCE COMPARISON BETWEEN CONVENTIONAL AND PROPOSED FILTERS DESIGNED BY THE EXISTING AND COMBINED OPTIMIZATION METHOD (DB). (CONV.: CONVENTIONAL ARCHITECTURE, PROP.: PROPOSED ARCHITECTURE)

Filter # [2]		$12A$	$16B$	$24F$	$32C$	$32E$	$48E$	$64E$
M		3	3	2	3	2	2	3
ideal		57.92	51.42	38.37	57.26	25.04	31.61	39.39
rounding	conv.	43.84	40.53	30.19	41.25	27.91	27.43	33.72
	prop.	53.7	49.72	36.09	48.23	25.04	28.55	37.84
local opt. [8]	conv.	56.01	47.79	34.15	46.36	28.76	31.24	37.28
	prop.	57.58	50.82	39.37	53.68	28.9	33.41	41.03
genetic alg. [11]	conv.	54.51	47.26	31.13	43.10	28.76	31.36	34.55
	prop.	60.28	52.91	40.04	51.93	29.45	34.32	36.04
local + gen. [Sec.3.3]	conv.	55.49	50.32	34.15	46.36	28.76	32.67	37.81
	prop.	60.28	53.40	40.04	56.30	29.61	34.75	40.16

Table III shows the performance comparison between the conventional and proposed SPT design. Various low pass filters denoted in [2] have been simulated using simple rounding, local optimization [8], genetic algorithm [11], and proposed algorithm. It can be observed that the maximum stopband attenuation of proposed architecture is higher than that of the conventional design in most cases. Also, the proposed optimization technique shows a better design result than using only local optimization or genetic algorithm.

V. CONCLUSION

We have proposed an architecture for the PR QMF lattice with SPT coefficients. The proposed method splits each stage into cascade of rotations that are implemented by CORDIC, whereas the conventional approach directly quantizes each coefficient into SPT form. By this cascade structure, the number of candidate discrete angles increases and thus the quantization error is reduced. An optimization technique, which is the combination of existing local and genetic algorithm, is also proposed for the search of suboptimal coefficients of the proposed and conventional filters. We have designed various QMF lattice filters using the conventional and combined design techniques, and the comparison shows that the proposed architecture with the new design algorithm provides larger stopband attenuation than the existing designs.

REFERENCES

[1] P. P. Vaidyanathan, *Multirate Systems and Filter Banks*. Englewood Cliffs, NJ: Prentice-Hall, 1993.
[2] P. P. Vaidyanathan and P. Q. Hoang, "Lattice structures for optimal design and robust implementation of two-channel perfect-reconstruction QMF banks," *IEEE Trans. Acoust., Speech, Signal Process.*, vol. 36, no. 1, pp. 81–94, Jan. 1988.
[3] T. Q. Nguyen and P. P. Vaidyanathan, "Two-channel perfect-reconstruction FIR QMF structures which yield linear-phase analysis and synthesis filters," *IEEE Trans. Acoust., Speech, Signal Process.*, vol. 37, no. 5, pp. 676–690, May 1989.
[4] C. K. Goh and Y. C. Lim, "An efficient algorithm to design perfect reconstruction regular quadrature mirror filters using weighted L_p error criteria," in *Proc. IEEE ISCAS'98*, May 1998, vol. 5, pp. 158–161.

[5] C. K. S. Pun, S. C. Chan, and K. L. Ho, "Efficient design of a class of multiplier-less perfect reconstruction two-channel banks and wavelets with prescribed output accuracy," in *Proc. IEEE Signal Process. Workshop Statistical Signal Process.*, Aug. 2001, pp. 599–602.
[6] Y. C. Lim and Y. J. Yu, "A width-recursive depth-first tree search approach for the design of discrete coefficient perfect reconstruction lattice filter bank," *IEEE Trans. Circuits Syst. I, Fundam. Theory Appl.*, vol. 50, no. 6, pp. 257–266, Jun. 2003.
[7] ——, "A successive reoptimization approach for the design of discrete coefficient perfect reconstruction lattice filter bank," in *Proc. IEEE ISCAS'00*, May 2000, vol. 2, pp. 67–92.
[8] B. R. Horng, H. Samueli, and A. N. Willson, Jr., "The design of two-channel lattice-structure perfect-reconstruction filter banks using powers-of-two coefficients," *IEEE Trans. Circuits Syst. I, Fundam. Theory Appl.*, vol. 40, no. 7, pp. 497–499, Jul. 1993.
[9] J. Y. Kaakinen, T. Saramaki, and R. Bregovic, "An algorithm for the design of multiplierless two-channel perfect reconstruction orthogonal lattice filter banks," in *Proc. 2004 1st Int. Symp. Contr., Commun., Signal Process.*, Mar. 2004, pp. 415–418.
[10] S. Sriranganathan, D. R. Bull, and D. W. Redmill, "The design of low complexity two-channel lattice-structure perfect-reconstruction filter banks using genetic algorithms," in *Proc. IEEE ISCAS'97*, May 1996, vol. 4, pp. 762–765.
[11] Y. J. Yu and Y. C. Lim, "New natural selection process and chromosome encoding for the design of multiplierless lattice QMF using genetic algorithm," in *Proc. IEEE ICECS'01*, Sep. 2001, vol. 3, pp. 1273–1276.
[12] S. Y. Park and N. I. Cho, "Design of perfect reconstruction QMF lattice with signed powers-of-two coefficients using CORDIC algorithm," in *Proc. IEEE ICASSP'05*, Mar. 2005, vol. 4, pp. 565–568.
[13] Y. C. Lim and S. R. Parker, "FIR filter design over a discrete power-of-two coefficient space," *IEEE Trans. Acoust., Speech, Signal Process.*, vol. ASSP-31, no. 3, pp. 583–591, Jun. 1983.
[14] H. Samueli, "An improved search algorithm for the design of multiplierless FIR filters with powers-of-two coefficients," *IEEE Trans. Circuits Syst.*, vol. 36, no. 7, pp. 1044–1047, Jul. 1989.
[15] S. C. Chan, W. Liu, and K. L. Ho, "Multiplierless perfect reconstruction modulated filter banks with sum-of-powers-of-two coefficients," *IEEE Signal Process. Lett.*, vol. 8, no. 6, pp. 163–166, Jun. 2001.
[16] J. Volder, "The CORDIC trigonometric computing technique," *IRE Trans. Electron. Comput.*, vol. EC-8, no. 3, pp. 330–334, Sep. 1959.
[17] J. S. Walther, "A unified algorithm for elementary functions," in *Spring Joint Computer Conf.*, 1971, vol. 38, pp. 379–385.
[18] C. S. Wu and A. Y. Wu, "Modified vector rotational CORDIC (MVR-CORDIC) algorithm and architecture," *IEEE Trans. Circuits Syst. II, Analog Digit. Signal Process.*, vol. 48, no. 6, pp. 548–561, Jun. 2001.
[19] C. S. Wu, A. Y. Wu, and C. H. Lin, "A high-performance/low-latency vector rotational CORDIC architecture based on extended elementary angle set and trellis-based searching schemes," *IEEE Trans. Circuits Syst. II, Analog Digit. Signal Process.*, vol. 50, no. 9, pp. 589–601, Sep. 2003.
[20] A. Y. Wu and C. S. Wu, "A unified view for vector rotational CORDIC algorithms and architectures based on angle quantization approach," *IEEE Trans. Circuits Syst. I, Fundam. Theory Appl.*, vol. 49, no. 10, pp. 1442–1456, Oct. 2002.
[21] A. Y. Wu, I. H. Lee, and C. S. Wu, "Angle quantization approach for lattice IIR filter implementation and its trellis de-allocation algorithm," in *Proc. IEEE ICASSP'03*, Apr. 2003, vol. 2, pp. 673–676.
[22] P. Rieder, J. Gotze, J. A. Nossek, and C. S. Burrus, "Parameterization of orthogonal wavelet transforms and their implementation," in *Proc. IEEE ICASSP'03*, Apr. 2003, vol. 2, pp. 673–676.
[23] S. Y. Park and N. I. Cho, "Fixed-point error analysis of CORDIC processor based on the variance propagation formula," *IEEE Trans. Circuits Syst. I, Fundam. Theory Appl.*, vol. 51, no. 3, pp. 573–584, Mar. 2004.
[24] Y. H. Hu, "The quantization effects of the CORDIC algorithm," *IEEE Trans. Signal Process.*, vol. 40, no. 4, pp. 834–844, Apr. 1992.

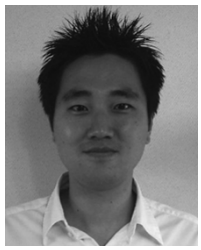

Sang Yoon Park was born in DaeGu, Korea, on December 25, 1976. He received the B.S. and M.S. degrees in electrical engineering from Seoul National University, Seoul, Korea, in 2000 and 2002, respectively. He is currently working toward the Ph.D. degree in electrical engineering at Seoul National University.

His research interests include design and implementation of signal processing systems.

Nam Ik Cho received the B.S., M.S., and Ph.D. degrees in control and instrumentation engineering from Seoul National University, Seoul, Korea, in 1986, 1988, and 1992, respectively.

From 1991 to 1993, he was a Research Associate of the Engineering Research Center for Advanced Control and Instrumentation, Seoul National University. From 1994 to 1998, he was with the University of Seoul, Seoul, Korea, as an Assistant Professor of Electrical Engineering. He joined the School of Electrical Engineering, Seoul National University, in 1999, where he is currently an Associate Professor. His research interests include speech, image, video signal processing, and adaptive filtering.